Fifteen years of experience with the estimation of structural loadings acting on temporary supports of tunnels in Buenos Aires

E. Núñez
University of Buenos Aires, Argentina.

A. O. Sfriso & J. G. Laiún
University of Buenos Aires and SRK Consulting, Argentina.

ABSTRACT: In 1998, shotcrete was used for the temporary support of a subway tunnel for the first time in Buenos Aires. The first author, consultant for the contractor, had developed a semiempirical method for the estimation of the structural support loads and used it to design the tunnel. The second author performed FEM models of the same tunnel and studied the effect of various variables, including construction stages and shotcrete thickness. By that time, a surprisingly good agreement was found between the structural loads obtained by the simple method and by the FEM models. 15 years later, both methods have been employed for the design of some 15km of tunnels. The agreement between the results given by the formulas and the numerical models was confirmed in most cases. In this paper, the derivation of the semi-empirical method is revisited; the results obtained for seven tunnels is compared to numerical estimates, and the differences are discussed.

Keywords: NATM tunnels, structural loadings, closed-form solution, numerical methods.

1 INTRODUCTION

The City of Buenos Aires is expanding it's metro network as shown in Figure 1. Recently completed and ongoing projects are: Line A, extended 5 km, Line B, extended 5 km; Line E, extended 2 km; and new Line H, 5 km long. Some 20 km of new Lines F, G, I are scheduled for construction in the near future). Landmarks of new construction procedures for tunnels are (Sfriso 2008): i) introduction of shotcrete, Line B, 1998; ii) so called "belgian" tunneling method, Line H, 2000; iii) full face excavation, Line B, 2004.

The first shotcrete-lined tunnel was a single lane tunnel in Line B, excavated using the german method of tunnelling (Figure 2). The first author, acting as the tunnel designer, estimated the lining loads using semi-empirical formulas he had derived some time ago (Núñez 1996). The second author performed finite-element analyses which resulted in surprisingly good agreement to the closed-form estimates.

Fifteen years later, the use of Núñez's formulas and numerical methods is routine practice and have been eployed for the preliminary and final design of some 15km of tunnels.

Unfortunately, field measurement of structural loads was never performed in these tunnels; the only reliable indication of the quality of the predictions is the concordance between the measured and computed surface and crown settlements. However, the similitude of the structural loads computed using the closed-form and numerical solutions was confirmed in many cases.

In this paper, the original derivation of the closed-form solution is reproduced (Núñez 1996) and the comparison between the closed-form solution and the numerical computations for lining loads are shown for several projects.

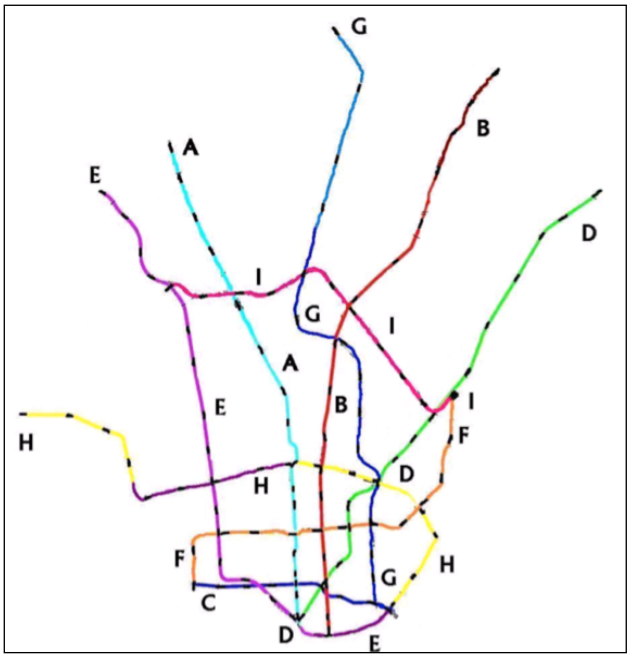

Figure. 1. Metro network in Buenos Aires. Existing (A, B, C, D, E, H) and new projects (F, G, I).

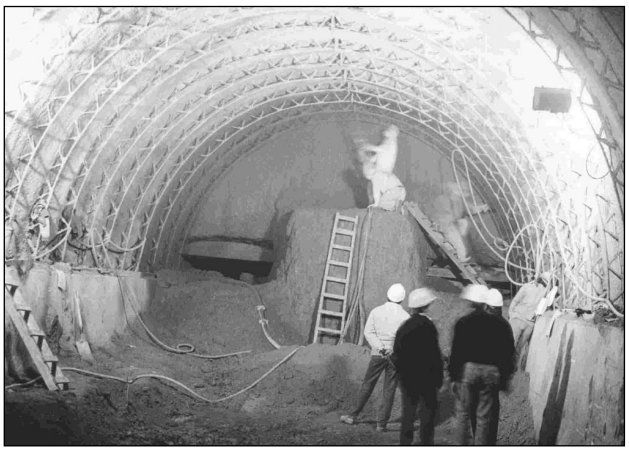

Figure 2. German method of tunneling and first use of shotcrete, Line B, 1998.

2 GEOTECHNICAL CONDITIONS IN BUENOS AIRES CITY

2.1 *Description*

Buenos Aires City lays on the Pampeano Formation, a large cuaternary sedimentary basin composed by stiff and hard silts and clays of eolic origin and genetically classified as a loess loam. The formation is a high terrace that forms 400km of the west coast of the Paraná and River Plate rivers, starting north of Rosario, Santa Fé, and ending south of Magdalena, Buenos Aires (Bolognesi 1975, Fidalgo et al 1975, Núñez 1986, Bolognesi & Vardé 1991).

Post depositional drying-wetting cycles imposed distinct morphological characteristics to the soil mass: fissures inducing secondary permeability, cementation produced precipitation of calcium carbonates and manganese oxides, and the growth of medium to large carbonate blocks showing a highly cemented matrix, locally called “toscas”.

2.2 *Mechanical behavior*

The mechanical behavior of the Pampeano soils has been described elsewhere (Núñez 1986, Núñez & Micucci 1986). The most distinctive characteristic is cementation: the drained un-confined compression strength q_u is frequently in the range 150kPa to 300kPa but can be more than 1000kPa for highly cemented “toscas”.

Strongly fissured regions resemble a well imbricated set of polyedra, a few centimeters wide, and showing the behavior of a highly jointed weak rock mass.

It is experimentally observed that the secant Young’s modulus varies linearly with stress mobilisation

$$E_s = E_i \cdot \left(1 - d_r \cdot (\sigma_1 - \sigma_3)/\sigma_R\right) \quad (1)$$

where $d_R \sim 0.8$ to 0.9, σ_1 and σ_3 are the major and minor principal stresses, σ_R is the soil strength E_i is the initial Young’s modulus, which correlates with the unconfined compression strength

$$E_i = 300 \cdot q_u \pm 30\% \quad (2)$$

This set of expressions has been published for the first time as part of course notes at the University of Buenos Aires in the late ’60s (Figure 3) and reproduced in the Casagrande Lecture (Núñez 2007).

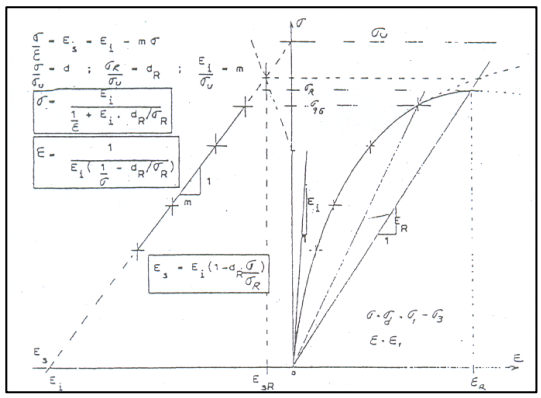

Figure 3. Stress-strain behavior of Pampeano Soils (course notes at University of Buenos Aires).

Except for the heaved upper three to six meters, penetration resistance is systematically N_{SPT} > 20 with some heavily cemented zones where N_{SPT} >> 50.

The secondary permeability of the soil mass is in the range 10^{-4}cm/s to 10^{-5}cm/seg, depending on the spacing and width of the fissures. Close to the bottom of the formation and right on top of pliocene clean sands, a poorly cemented, non-fissured sub-stratum of greenish clays acts as an hydraulic seal.

2.3 *Material parameters for numerical modelling*

Table 1 shows a typical set of material parameters used in the numerical modelling of tunnelling projects where the Hardening Soil Model available in Plaxis is employed (Codevilla & Sfriso 2011). Stress-strain relationships of the HSM model are reproduced in Eqs. 3a to 3d.

Table 1. Design material pars, Pampeano Formation.

Parameter	Units	0m-8m	8m-30m	30m-40m
c_u	kPa	50-100	110-220	40-120
ϕ_u	°	10-20	0-10	0
c'	kPa	10-25	25-50	15-30
ϕ'	°	30-32	30-34	29-32
ψ	°	0-3	0-6	0-3
E_{50}^{ref}	MPa	60-100	70-150	60-90
E_{ur}^{ref}	MPa	150-250	180-300	140-220
m	-	0.0-0.4	0.0-0.4	0.0-0.4
ν	-	0.20-0.30	0.20-0.30	0.20-0.30
R_f	-	0.80-0.90	0.80-0.90	0.80-0.90

$$\sigma_1 - \sigma_3 = \begin{cases} \text{load: } 2E_{50}\left(1 - R_f \dfrac{\sigma_1 - \sigma_3}{\sigma_3 N_\phi + 2c\sqrt{N_\phi}}\right)\varepsilon_1 \\ \text{unload: } E_{ur}\varepsilon_1 \end{cases} \quad (3a)$$

$$N_\phi = \tan^2\left[\frac{\pi}{4} + \frac{\phi}{2}\right] \quad (3b)$$

$$E_{ur} = E_{ur}^{ref}\left(\frac{\sigma_3 + c\cot[\phi]}{c\cot[\phi] + p_{atm}}\right)^m \quad (3c)$$

$$E_{50} = E_{50}^{ref}\left(\frac{\sigma_3 + c\cot[\phi]}{c\cot[\phi] + p_{atm}}\right)^m \quad (3d)$$

In Eqs. 3a to 3d and Table 1, ε_1 is the major principal strain, c is the cohesion, ϕ is the friction angle, ψ is the dilatancy angle, E_{50}^{ref} and E_{ur}^{ref} are the reference loading/unloading Young's moduli, m is a stiffness exponent, ν is the Poisson's ratio and R_f is the failure ratio.

2.4 *Behavior in underground works*

Pampeano soils are favourable materials for underground construction due to their high stiffness, reliable compression strength, rapid drainage and good frictional behavior when drained. However, the existence of a systematic fissuring implies that there is always a risk of localized failure of vertical unsupported cuts or long unsupported tunnel drifts.

The experience accumulated during the last fifteen years is that the maximum allowable unsupported drift is about 2.5m to 3.0m, not limited by convergence or plastic deformations but by the risk of occurrence of cone-shaped, localized crown instabilities (Núñez 1996, 2007, Sfriso 2006, 2008).

Fissures and cementation can vary strongly in short distances; therefore, the observational method is the best approach for efficient and economic tunnelling in these soils, where judgement is applied at the face to adjust the unsupported drift to soil conditions.

An indicator of face stability in tunnelling is usually computed using the expression

$$F = (\gamma \cdot H + q)/s_u \quad (4)$$

where γ is soil's unit weight, H is the overburden, q is the surface load and s_u is the undrained shear strength. A critical value F > 6.0 means potential face instability.

No incidentes related to face instability have been reported at any of the many single and double lane tunnels excavated in the last 15 years, nor for underground caverns.

3 A SEMI-EMPIRICAL CLOSED-FORM SOLUTION FOR STRUCTURAL LOADING OF LININGS

3.1 *Typical support systems*

The typical support system for NATM tunnels in Buenos Aires employs lattice girders, wire mesh and shotcrete. In some cases, lattice girders outcrop from the primary support to connect it to the permanent lining. In most cases, however, lattice girders are completely covered by shotcrete and both liners are assumed to work independently.

Cement grouting, anchors, bolts, pre-excavation support methods and face support methods are not used in Buenos Aires tunnelling and shall not be analysed here.

3.2 *Basic hypotheses*

The nomenclature is: D is the diameter of the tunnel, r_0 the radius, H the overburden (surface to tunnel axis); e is the shotcrete thickness, E_r is the shotcrete Young's modulus, E_s is the soil's Young modulus, ν_r is the shotcrete Poisson's ratio, ν_s is the soil's Poisson's ratio, σ_v is vertical pressure at the tunnel axis and K_0 is the soil's at-rest stress ratio.

Conventional tunnel analysis assumes that the excavation of a circular horizontal tunnel produces a convergence displacement of the soil mass into the cavity. A plastic crown of radius r_e is formed if the soil strength is fully mobilized in the vicinity of the excavation.

If no support is placed in the tunnel, the radial pressure acting against the excavated surface is zero. For this particular case, the relationship between the plastic radius and the tunnel radius is (Westergaard 1940)

$$\frac{r_e}{r_0}=\left[\frac{2}{N_\phi-1}\cdot\left(\left(N_\phi-1\right)\cdot\frac{\sigma_v}{q_u}+1\right)\right]^{\frac{1}{N_\phi-1}} \tag{5}$$

Typical metro tunnels in Buenos Aires have overburdens of one to two tunnel diameters and typical r_e/r_0 ratios of 1.4 +/-15%. For 10m diameter tunnels, the plastic crown is some 2m thick. As described before, the soil does not allow for unsupported tunnelling due to the fissure-induced crown instabilities.

3.3 *Stress relaxation due to tunnelling*

Where no water pressures act on the tunnel and for isotropic stress state, the radial stress σ_{r0} at the tunnel axis equals the vertical pressure

$$\sigma_v=\gamma H+q \tag{6}$$

When the face advances, a stress relaxation occurs and the radial stress is reduced to

$$\sigma_{r0}=\eta\cdot\sigma_v \tag{7}$$

where η is a stress-relaxation coefficient.

Due to the above-mentioned effect of soil fissures, shotcrete is applied inmediately after the excavation. This effectively reduces the development of a plastic crown to a minimum; soil largely remains in an elastic state.

Therefore, the stress-relaxation coefficient η can be computed to match the computed behavior of an elastic soil: $1.5r_0$ behind the analysis section, no stress relaxation occurrs, and then η = 1; at the analysis section, partial stress relaxation is predicted. Depending on various parameters, η can be computed to be in the range 0.60 to 0.67; when the face is $3r_0$ beyond the analysis section, full relaxation occurs, and η = 0. The following simple linear formula is adopted

$$\eta=2/3\cdot\left(1-1/3\cdot d/r_o\right) \tag{8}$$

where d is the distance between the analysis section and the tunnel face. Eq. 8, of course, limits the validity of the whole procedure to tunnels in hard soils exhibiting little yielding.

The stress field around the tunnel can be splitted in two parts: an isotropic stress field producing compression of the lining only

$$\sigma_v^{(1)}=\sigma_h=K_0\cdot\eta\cdot\sigma_v \tag{9}$$

where σ_h is the horizontal stress, and a vertical stress field inducing both compression and bending stresses

$$\sigma_v^{(2)}=\left(1-K_0\right)\cdot\eta\cdot\sigma_v \tag{10}$$

3.4 *Strength mobilisation*

A classical approach to strength mobilisation is shown in Figure 4 (adapted from Terzaghi 1943). Vertical pressure acting on the plane a-a is reduced by the shear stresses acting on the vertical sides of the mobilised soil mass. For instance, a tunnel having H = 15m and D = 10m yields B ~16m. Assuming a mean shear strength s = 80kPa, the vertical pressure acting on the tunnel crown is

$$\sigma_v=\left(\gamma\cdot B-2\cdot s\right)\cdot\left(H-D/2\right)=100\text{kPa} \tag{11}$$

which implies a reduction of 66% of the overburden pressure given by Eq. 6. Factors 33% to 66% are common in Buenos Aires tunnels.

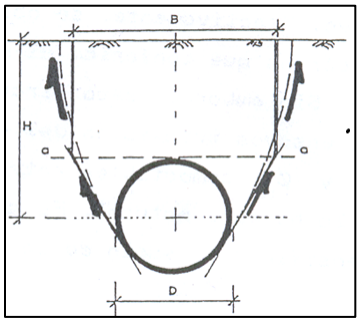

Figure 4. Shear stresses reducing the effective vertical pressure acting on the crown (After Terzhaghi 1943).

3.5 *Induced displacements in the soil mass*

Long behind the tunnel face, 2D plane strain conditions apply. Radial displacements at the elastic crown can be then computed using

$$u_{re} = (\sigma_{r0} - \sigma_{re}) \cdot (1 + \nu_s) / E_s \cdot r_e \tag{12}$$

Isochoric deformation is assumed for the plastic crown. Therefore, the radial displacement at the tunnel walls can ve estimated using

$$u_{r0} = (\sigma_{r0} - \sigma_{re}) \cdot (1 + \nu_s) / E_s \cdot (r_e / r_o)^2 \cdot r_e \tag{13}$$

It is fully acknowledged that this is a simplified approach, as the actual stress path involves unloading in the radial direction and plastic loading in the circunferential direction, and therefore the use of a constant Young's modulus is not accurate.

3.6 *Displacements of an elastic tube*

The circular support is analyzed using classic formulas for an elastic tubes in 2D plane strain. The plane strain constrained modulus apply both for soil and lining

$$\begin{aligned} E_{r0} &= E_r / (1 - \nu_r^2) \\ E_{s0} &= E_s / (1 - \nu_s^2) \end{aligned} \tag{14}$$

The stress field described in Eq. 10 yields an outwards horizontal displacement of the tube which can be computed using the expression

$$u_h = (\sigma_v - \sigma_h) \cdot r_o^4 / (6 \cdot E_{r0} \cdot I) \tag{15}$$

This displacement based on the response of an elastic tube interacts with that of Eq. 13 as follows.

3.7 *Soil-structure interaction*

Soil-structure interaction can be conceptually studied by the convergence-confinement curve, as shown in Figure 5. The σ_{r0}–u_{r0} line is a curve even in the so-called elastic state because the soil's Young's modulus is not constant (see Eq. 1). For practical purposes, however, the curve A-B-C is replaced by the straight line A-C.

The effect of confinement can be readily incorporated using the subgrade reaction concept and computing the pressure induced by a horizontal displacement with

$$\sigma_h = K \cdot u_h \tag{16}$$

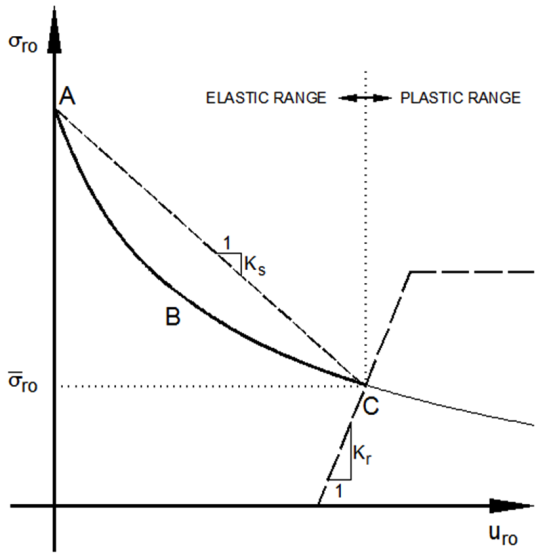

Figure 5. Convergence-confinement curve.

where K is a "subgrade modulus" defined as

$$K = \chi \cdot E_{s0} / D \tag{17}$$

and χ is an adjustment factor that depends on the roughness of the contact between soil and lining. For smooth contacts, the normal stress exerted by the lining against the soil is rather uniform. For rough contacts, lining deformation induces a stress field which shows a higher stress concentration close to the equator of the lining (equivalent to a smaller contact area). A value χ = 1.0 is recommended for a smooth lining and χ = 2.0 for a rough lining.

Replacing Eqs. 15 in Eq. 16 and solving por σ_h yields

$$\sigma_h = \sigma_v \Big/ \left(1 + \frac{12 \cdot E_{r0} \cdot I}{K \cdot r_o^4} \right) \tag{18}$$

The final pressure difference acting on the tube accounting soil-structure interaction is then

$$\sigma_v - \sigma_h = \left(1 - \frac{1}{\left(1 + (12 \cdot E_{r0} \cdot I) / K \cdot r_o^4\right)} \right) \sigma_v \tag{19}$$

Taking into account that $I = e^3/12$, this equation can be put in the short form

$$\begin{aligned} \sigma_v - \sigma_h &= \frac{a}{1+a} p_v \\ a &= 16 \frac{E_{r0}}{\chi \cdot E_{s0}} \frac{1 - \nu_s^2}{1 - \nu_r^2} \left(\frac{e}{D} \right)^3 \end{aligned} \tag{20}$$

In Eq. 20, χ = 1.0 is recommended for primary supports and χ = 2.0 for permanent linings.

3.8 *Structural loads*

According to elasticity theory for circular tubes, the bending moment produced by the pressure difference is

$$M_{\max} = \frac{1}{16} \cdot (\sigma_v - \sigma_h) \cdot D^2 \quad (21)$$

Combining Eqs. 6, 20 and 21 and operating yields (Figure 6) (Núñez 1996)

$$M_{\max} = \frac{1}{16} \cdot \eta \cdot (1 - K_0) \cdot (\gamma \cdot H + q) \cdot D^2 \cdot \frac{a}{1+a} \quad (22)$$

which is the final expression for the positive bending moment at the crown of the tunnel and for the negative bending moment at the tunnel's equators. In Eq. 22, η = 1/3 to η = 2/3 is recommended for primary supports and η = 1.0 for permanent linings (Núñez 1996).

The normal load acting at the equator of the tunnel can be evaluated as one half of the vertical acting load, namely

$$N_A = ½ \cdot \eta \cdot D \cdot (\gamma \cdot H + q) \quad (23)$$

For the computation of the normal load at the crown, both the pressure difference between crown and invert and K_0 must be taken into consideration. As a rough conservative estimate, it can be considered that 1/3 of the total horizontal load is taken by the crown, and 2/3 by the invert. After some algebra, the normal load at the crown is (Núñez 1996)

$$N_C = \frac{1}{2} \eta \cdot D \cdot (\gamma \cdot H + q) \cdot \left(K_0 + \frac{2}{3} \frac{1 - K_0}{1+a} \right) - \frac{1}{12} K_0 \cdot \gamma \cdot D^2 \quad (24)$$

Similarly, the normal load at the invert is computed with the expression (Núñez 1996)

$$N_I = \frac{1}{2} \eta \cdot D \cdot (\gamma \cdot H + q) \cdot \left(K_0 + \frac{4}{3} \frac{1 - K_0}{1+a} \right) + \frac{1}{12} K_0 \cdot \gamma \cdot D^2 \quad (25)$$

4 NUMERICAL MODELLING

4.1 *Background*

Numerical methods have been systematically employed for the design of metro tunnels and caverns in Buenos Aires. Both 2D and 3D models have been developed and have been reported in a number of publications (Sfriso 1999, 2006, 2007, 2008, 2010, Sfriso & Laiún 2012).

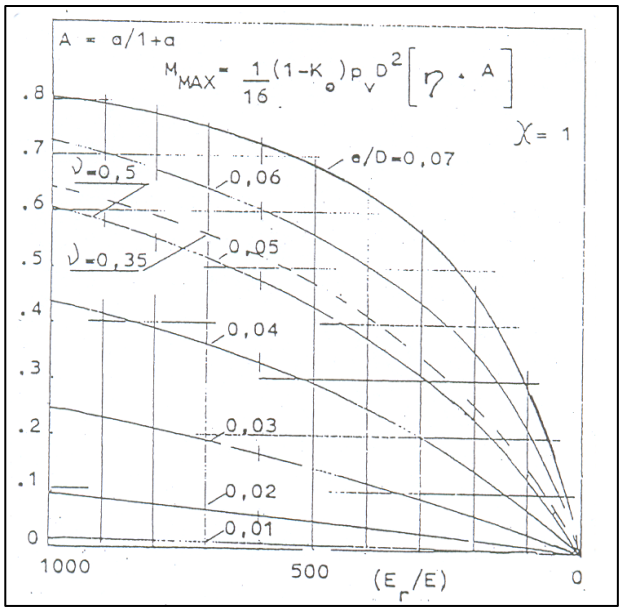

Figure 6. Chart for the computation of maximum bending moment in the crown of a circular tunnel.

The Hardening Soil Model available in Plaxis has been employed in all cases, and has been calibrated upon the accumulated experience. The most recent set is that shown in Table 1 (Codevilla & Sfriso 2011).

4.2 *Selected sections*

Out of a +50 tunnels and caverns designed using both numerical methods and the semi-empirical expressions introduced above, a small subset of seven tunnels has been selected for comparison purposes.

The selected sections cover the vast majority of cases regarding tunnel diameter ($0.5D < H < 1.5D$), width ($5.5\text{m} < B < 20.0\text{m}$), soil conditions ($20 < N_{SPT} < +50$), shape (one lane, two lanes, caverns) and construction procedures (german, belgian and full-face methods of excavation).

No invert is usually built close to the tunnel face except where uplift pressures exist from underlying sand lenses or where settlements must be reduced for environmental reasons. Open rings can be taken into account in the numerical models but not in the closed-form expressions, and therefore no "exact" matching should be expected in most cases.

Table 2. Key parameters for seven selected tunnels.

#	H [m]	D [m]	d [m]	e [m]	q [kPa]	K_0	η	E_{s0} [MPa]
1	18.0	10.0	7.0	0.15	20	0.60	0.50	180
2	15.9	5.45	4.8	0.10	12	0.60	0.50	240
3	11.9	17.4	9.4	0.25	12	0.60	0.50	180
4	13.4	18.7	14.0	0.30	12	0.60	0.67	180
5	4.9	5.5	4.8	0.10	12	0.60	0.67	240
6	18.0	10.0	7.0	0.15	20	0.60	0.67	180
7	14.6	18.0	10.0	0.25	20	0.60	0.67	180

5 COMPARISON OF DESIGN METHODS

5.1 *Comparison of structural loads*

Table 3 shows the results obtained using both the closed-form expressions and the numerical models. Cases 1 to 3 are horse-shoe sections with no invert. For these cases, η = 0.50 is usually adopted. Cases 4 to 7 had inverts built close to the tunnel face, and η = 0.67 was adopted then.

Table 3. Comparison of structural loads for seven tunnels: close-form solution (left) vs. FEM computations (right).

#	N_c [kN/m]	N_a [kN/m]	M_c [kNm/m]	M_a [kNm/m]
1	620|740	670|615	4.8|2.2	5.9|6.5
2	365|380	450|385	1.5|0.5	1.6|1.6
3	720|500	680|780	10.2|10.0	13.8|65.0
4	1080|1070	1180|600	17.0|8.0	21.0|35.0
5	120|110	160|125	0.5|0.5	0.5|0.9
6	825|905	870|955	6.4|2.0	7.9|2.5
7	1070|985	1025|1235	18.0|6.9	24.2|67.0

Table 4 shows the same data but in ratio form (analytical / numerical). Figures lower than 1.0 indicate that the closed-form solution under-estimates the load, if the FE results are to be accepted as accurate.

Table 4. Comparison of structural loads for seven tunnels: ratio of close-form solution to FEM computations.

#	N_c -	N_a -	M_c -	M_a -
1	0.84	1.09	2.18	0.91
2	0.96	1.17	3.00	1.00
3	1.44	0.87	1.02	0.21
4	1.01	1.97	2.13	0.60
5	1.09	1.28	1.00	0.56
6	0.91	0.91	3.20	3.16
7	1.09	0.83	2.61	0.36

Good agreeement is found for normal loads. For bending moments, scatter is somewhat higher and in some cases the figures are quite different.

5.2 *Analysis*

Drilling down into the data, it is observed that the max departure occurs in cases 4 and 7. Case 4 is Corrientes Station, Case 7 is the Line A warehous. Both are large caverns excavated using bench-berm full-face techniques as shown in Figure 7 and Figure 8 (Sfriso 2007).

A second contributor to the scatter is stratighraphy. For large caverns, it is always the case that the upper part of the section lies in medium-stiff clayley soils while the bottom part lies in much stiffer soils. While this is properly taken into account in the numerical models, it is not considered at all in the closed-form expressions.

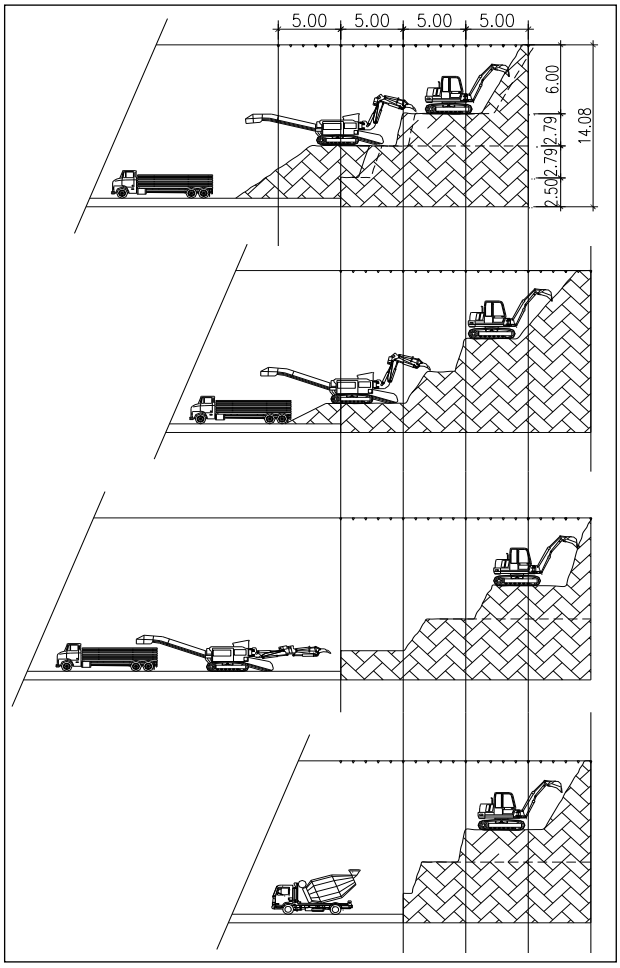

Figure 7. Construction stages of Case 4, Corrientes Station (Sfriso 2007).

The set of equations 22 to 25 provide an explicit set of formulas to readily compute structural loadings on tunnels. Sfriso (1996) and Núñez (2007) reported that loads computed using these equations compare within 10% − 15% with those computed using the Einstein – Schwarz procedure (Einstein & Schwartz 1979).

Figure 8. Face view of Case 4, Corrientes Station (Sfriso 2007).

Núñez (2000) presented an extended version of the closed-form solution presented here. In this extended version he accounted for elliptical shapes and water pressures. This extended version, however, adds little accuracy to the predictions, as the main driver for the scatter is the effect of construction procedures, which lies beyond the scope of any analytical approach.

6 CONCLUDING REMARKS

In this paper, the hypotheses and derivation of the semi-empirical closed-form expressions for the estimation of structural loads on tunnels, originally proposed by Núñez (1996) was revisited.

The usefulness of a closed-form expressions is evident, as they provide an easy and robust way to: i) define the minimum thickness of shotcrete; ii) define reinforcing / girder weight and spacing; and iii) provide a tool to check the reasonability of the results of involved numerical models.

The set of Eqs. 22 to 25 provide an easy way to estimate structural loads on tunnels excavated in stiff soils like Buenos Aires soils. When compared against Einstein & Schwartz (1979) solution, a small scatter in the range 10% - 15% is observed. When compared against seven typical tunnel designed using finite element procedures, the scatter is shown to be higher and dependent on the construction procedure used to excavate the tunnel. Nevertheless, the usefulness of the approach is demonstrated by it's continued application in practical tunnel engineering in Buenos Aires for the last 15 years.

REFERENCES

Bolognesi A, 1975. Compresibilidad de los suelos de la Formación Pampeano. V PCSMFE, Argentina, V: 255-302.

Bolognesi A and Vardé O, 1991. Subterráneos en Buenos Aires. IX PCSMFE, Chile, III:1329-1350.

Codevilla M and Sfriso A, 2011. Actualización de la información geotécnica de los suelos de la Ciudad de Buenos Aires. XIV PCSMGE (Toronto, Canadá), paper 988 , CD-ROM.

Einstein H and Schwartz C, 1979. Simplified analysis for tunnel supports. ASCE Journal Geotech Eng Div 104(4):499–518.

Fidalgo F, De Francesco F and Pascual R, 1975. Geología superficial de la llanura Bonaerense". VI Arg. Geol. Conf, 110 - 147.

Núñez E, 1986. Panel Report: Geotechnical conditions in Buenos Aires City. V Conf. IAEG, 2623-2630.

Núñez E and Mucucci C, 1986b. Cemented preconsolidated soils as very weak rocks. V Conf. IAEG, 403-410.

Núñez E, 1996. Túneles de sección circular en la Formación Pampeano. Bull. SAMS, 29, 1-15.

Nuñez, E, 2000. Excavaciones y tuneles en el Pampeano, XV CAMSIG.

Núñez E, 2007. Casagrande lecture: Uncertainties and Approximations in Geotechnics. XIII PCSMGE, Venezuela.

Sfriso, A. 1996. Revestimiento de túnel circular: comentario. Bull. SAMS, 29, 16-20.

Sfriso A, 1999. Tunnels in Buenos Aires: Application of numerical methods to the structural design of linings. XI PCSMGE, Brasil, 637-642.

Sfriso A, 2006. Algunos procedimientos constructivos para la ejecución de túneles urbanos. XIII CAMSIG, Argentina, 1-17.

Sfriso A, 2007. Procedimiento constructivo de la Estación Corrientes del Subterráneo de Buenos Aires, Argentina. VI Cong Chil Geot, Valparaíso, d6:1-13.

Sfriso A, 2008. Metro tunnels in Buenos Aires: Design and construction procedures 1998 – 2007. 6th Intl Symp Geotechnical Aspects Underground Construction Soft Ground, Shanghai, 335-341.

Sfriso A, 2010. Metro tunnels in Buenos Aires. Development of construction procedures 1998-2009 (update). ITS Seminar, Buenos Aires, Argentina.

Sfriso A, Laiun J, 2012. Evolution of construction procedures for metro stations in Buenos Aires, Argentina. SAT 2012, San Pablo, Brasil.

Westergaard H, 1940. Plastic State of Stress around a Deep Well, J. Boston Soc. Civil Engr, 2, 1-5.